TÜBİTAK

Turkish Journal of Botany

http://journals.tubitak.gov.tr/botany/

Research Article

Turk J Bot
(2017) 41: 63-74
© TÜBİTAK
doi:10.3906/bot-1604-34

Studies on the floral anatomy and scent chemistry of titan arum (*Amorphophallus titanum*, Araceae)

Vijayasankar RAMAN[1,*], Nurhayat TABANCA[1,2], Betül DEMİRCİ[3], Ikhlas A. KHAN[1,4]

[1]National Center for Natural Products Research, School of Pharmacy, University of Mississippi, University, MS, USA
[2]Department of Entomology and Nematology, Emerging Pathogens Institute, University of Florida, Gainesville, FL, USA
[3]Department of Pharmacognosy, Faculty of Pharmacy, Anadolu University, Eskişehir, Turkey
[4]Division of Pharmacognosy, Department of Biomolecular Sciences, School of Pharmacy, University of Mississippi, University, MS, USA

Received: 21.04.2016 • **Accepted/Published Online:** 19.07.2016 • **Final Version:** 17.01.2017

Abstract: *Amorphophallus titanum* (Becc.) Becc. ex Arcang., the titan arum, is popularly known for having the world's largest unbranched inflorescence. The enormous flower-like inflorescence is also called 'corpse flower' or 'carrion flower' due to the characteristic putrid odor of the bloom. The present study illustrates detailed anatomy and micromorphology of the inflorescence by light and scanning electron microscopy. Collenchyma was found to be the major tissue providing mechanical support in the spathe. The appendix consisted of a dense parenchymatous cortex enclosing a hollow center traversed by loose networks of aerenchyma. Anthocyanin pigments found in the epidermises and cortical tissues imparted a purple color to various parts of the inflorescence. Two types of raphide crystals, *Psychotria* type and *Lemna* type, and cluster crystals were observed. The volatile compounds from different parts of the inflorescence were collected by a modified headspace-solid phase microextraction (HS-SPME) technique and the samples were analyzed by gas chromatography-mass spectrometry (GC-MS). The major volatile compounds found by this method included isovaleric acid (21.6%), butyric acid (17.0%), benzyl alcohol (16.2%), and γ-butyrolactone (12.1%) in the appendix; γ-butyrolactone (27.0%), tetradecane (13.4%), and 4-hydroxy-4-methyl-2-pentanone (10.5%) in the male flowers; tetradecane (19.9%), 4-hydroxy-4-methyl-2-pentanone (13.0%), and 3-hydroxy-2-butanone (10.6%) in the female flowers; and butyl acetate (44.5%) and 3-hydroxy-2-butanone (12.2%) in the spathe. Use of different types of SPME fibers and multiple analytical methods is necessary in order to obtain a complete picture of the volatile composition of titan arum blooms.

Key words: Titan arum, floral anatomy, microscopy, floral scent, headspace-solid phase microextraction, floral volatiles, biomimicry, pollination

1. Introduction

Titan arum (*Amorphophallus titanum* (Becc.) Becc. ex Arcang.) is well known for its enormous, spectacular inflorescence, which is the largest of its kind in the world. It is also widely known for its characteristic strongly unpleasant odor, due to which it is also called 'corpse flower' or 'carrion flower'. Endemic to Sumatra Island of Indonesia, the plant usually takes several years to bloom and the successive blooms happen only occasionally (Barthlott et al., 2009). It is rarely cultivated in botanical gardens and its blooming in cultivation is even rarer. This curious and rare plant has drawn the attention of botanists, chemists, and naturalists since its discovery.

The characteristic nauseating, strongly unpleasant odor of the titan arum bloom has always been intriguing although only a few studies have focused on the volatile chemistry behind this mystery. Using gas chromatography-mass spectrometry (GC-MS), Kite and Hetterschieid (1997) showed that dimethyl oligosulfides (75% dimethyl disulfide [DMDS] and 10% dimethyl trisulfide [DMTS]) were the main chemical components of the carrion smell of the inflorescence. They collected the odor during the female phase by positioning a trap (100 mm long × 3 mm diameter; SGE) packed with 100 mg of Tenax GR 35/60 near the appendix and drawing air through the trap using a portable pump. Shirasu et al. (2010) reported that the primary odorant causing the smell during anthesis was DMTS, a sulfur-smelling compound. Fujioka et al. (2012), using an electronic nose and standard gas descriptors, objectively described the carrion smell of *A. titanum* flowers as "decayed cabbage, garlic and pungent sour" and found that trimethylamine was responsible for the rotting-fish smell emitted at the end of flowering. Other compounds reported to contribute to the complex

* Correspondence: vraman@olemiss.edu

unpleasant odor include methyl thiolacetate, 3-methyl butanal, acetic acid, and isovaleric acid (Shirasu et al., 2010). During the present study, several additional compounds were observed by using a modified headspace-solid phase microextraction (HS-SPME) method. These odorants are collectively responsible for the putrid odor of the titan arum bloom.

Plant anatomy is fundamental to an understanding of various aspects of plants such as functional biology, metabolomics, ecology, and evolution. It is crucial for identification and characterization of plants and this subject has always been a backbone for phylogenetic classification of plants (Endress et al., 2000). Floral anatomies help understand the tissue differentiations and various functional adaptations of flowers in tune with the environmental conditions. Despite the incredible adaptations and interesting behaviors of titan arum, only a few publications on the detailed anatomy of this world's largest inflorescence (Barthlott and Lobin, 1998; Giordano, 1999) are available in the literature. This is probably due to the rarity of the plant and its flowering as well as difficulties in obtaining the material for research. Chapter 6 of the Barthlott and Lobin's publication (1998) provides an extensive account on the floral morphology and anatomy of titan arum although most parts of this and a few other chapters are written in German. There are few other papers that only deal with the vegetative anatomy (Hejnowicz, 2005; Hejnowicz and Barthlott, 2005) of titan arum. The scarcity of available literature on floral anatomy, as well as the recent blooming of two titan arum plants in our garden, encouraged us to conduct a detailed study of the anatomy of various parts of the inflorescence along with analysis of their scent chemistry. The present paper illustrates the floral anatomy of the titan arum by light and scanning electron microscopy (SEM).

2. Materials and methods

2.1. Plant materials

Several plants of titan arum, grown from seeds sown in 2008, are being maintained in the greenhouse facility at the Medicinal Plant Garden of the University of Mississippi, USA. Two of these plants flowered during 2014, and fresh specimens from these two inflorescences were used for the present study. The samples were assigned with unique accession numbers and were deposited in the botanical repository of the National Center for Natural Products Research (NCNPR), in the School of Pharmacy, University of Mississippi, MS, USA.

2.2. Preparation of samples for light microscopy

Freshly collected samples of titan arum floral parts were fixed in formalin-acetic acid-alcohol for 2 days and free-hand sections were prepared using razor blades. The sections were treated with chloral hydrate solution and stained with toluidine blue or phloroglucinol/HCl. Photomicrographs were prepared using Nikon E600 or Nikon E600 POL microscopes equipped with Nikon DS-Fiv camera systems and Nikon Elements imaging software (Nikon Inc., Tokyo, Japan).

2.3. Preparation of samples for scanning electron microscopy

Fresh samples were fixed overnight in 2.5% glutaraldehyde in 0.2 M sodium phosphate buffer (pH 7.4) and washed in distilled water. The fixed samples were dehydrated by passing through increasing concentrations of ethanol in water according to a standard method (Hayat, 2000). The dehydrated specimens were then dried in a critical point dryer (Denton Vacuum, Moorestown, NJ, USA) using liquid CO_2. The fully dried samples were then mounted on aluminum stubs using sticky carbon tabs and sputter-coated with gold (Hummer 6.2 sputter coater, Anatech USA, Union City, CA, USA). Digital images of the specimens were captured using a JSM-5600 Scanning Electron Microscope (JEOL USA Inc., Peabody, MS, USA).

2.4. HS-SPME

Freshly collected samples of titan arum (female flowers, male flowers, tissues from spathe, and appendix) were individually dried using Labconco Benchtop FreeZone Freeze-Dry Systems (Brentwood, NH, USA) before the HP-SPME-GC-MS analysis. The manual SPME device (Supelco, Bellefonte, PA, USA) with a fiber-precoated 65-μm-thick layer of polydimethylsiloxane/divinylbenzene (PDMS/DVB-blue) was used for absorption of the plant volatiles. The vial containing the plant samples was sealed with Parafilm. The fiber was pushed through the film layer for exposure to the headspace of the extract for 15 min at 40 °C. The fiber was then inserted immediately into the injection port of the GC-MS for desorption of the adsorbed volatile compounds for analysis (Tasdemir et al., 2003).

2.5. Analysis of volatile compounds

The volatiles were analyzed by GC-MS using an Agilent 5975 GC-MS system. An Innowax FSC column (60 × 0.25 mm, 0.25 μm film thickness) was used with helium as the carrier gas (0.8 mL/min). GC oven temperature was kept at 60 °C for 10 min and programmed to 220 °C at a rate of 4 °C/min, and kept constant at 220 °C for 10 min and then programmed to 240 °C at a rate of 1 °C/min. The injector temperature was set to 250 °C. Mass spectra were recorded at 70 eV. Mass range was *m/z* 35 to 450.

Identification of the volatile components was carried out by comparison of their relative retention times with those of authentic samples or by comparison of their relative retention index (RRI) to a series of *n*-alkanes. Computer database matching against commercial (Wiley GC/MS Library, MassFinder 3 Library) (McLafferty et al., 1989) and in-house 'Başer Library of Essential Oil Constituents'

built up by genuine compounds and components of known oils, as well as MS literature data (Joulain and König, 1998; ESO-2000, 1999), was used for the identification. Relative percentage amounts of the separated compounds were calculated from total ion current (TIC) chromatograms. The volatile compounds identified are listed in the Table.

3. Results

3.1. Observations of the blooms

Twenty-one titan arum plants are being grown in the greenhouse facility at the Maynard W. Quimby Medicinal Plant Garden of the University of Mississippi, USA. Two of these plants first flowered in 2014, one in mid-May and the

Table. Chemical composition of the floral scent of *Amorphophallus titanum*.

RRI	Compound	Appendix (%)	Male flower (%)	Female flower (%)	Spathe (%)	Identification
1087	Butyl acetate	-	-	-	44.5	MS
1296	3-Hydroxy-2-butanone	5.9	3.3	10.6	12.2	RRI, MS*
1300	Tridecane	-	-	4.4	-	RRI, MS
1374	4-Hydroxy-4-methyl-2-pentanone	2.9	10.5	13.0	2.0	RRI, MS*
1400	Tetradecane	-	13.4	19.9	2.0	RRI, MS
1400	Nonanal	2.4	0.1	-	-	MS
1409	Trimethyl pyrazine	1.8	-	-	-	MS
1496	2-Ethyl hexanol	0.1	2.0	7.7	0.7	MS
1541	Benzaldehyde	4.4	-	-	-	RRI, MS
1553	Linalool	-	2.1	-	-	RRI, MS
1631	Butyric acid	17.0	-	-	-	MS
1651	γ-Butyrolactone	12.1	27.0	0.1	-	MS
1685	Isovaleric acid	21.6	4.0	-	2.3	MS
1709	α-Terpinyl acetate	-	2.8	-	-	RRI, MS
1868	6-Methyl-γ-ionone	-	-	-	0.5	MS
1896	Benzylalcohol	16.2	6.1	3.0	0.9	RRI, MS
1925	Ionol	-	-	-	5.7	RRI, MS*
1945	Ionol 2	0.8	9.0	8.3	2.3	RRI, MS*
2033	Phenol	3.0	2.9	4.3	-	RRI, MS
2182	2-Phenoxyethanol	3.1	1.7	-	0.7	RRI, MS*
2308	Methyl dihydrojasmonate	-	-	-	2.4	MS
2500	Pentacosane	-	-	3.8	-	RRI, MS
2600	Hexacosane	-	-	5.1	-	RRI, MS
2700	Heptacosane	-	-	6.8	-	RRI, MS
2800	Octacosane	-	-	6.9	-	RRI, MS
	Total	91.3	84.9	93.9	76.2	

RRI - relative retention indices calculated against *n*-alkanes.
% - calculated from total ion current (TIC) data.
MS - identified on the basis of computer matching of the mass spectra with those of the Wiley and MassFinder libraries and comparison with literature data.
* - purchased from Sigma-Aldrich Co., St. Louis, MO, USA.

other in mid-June. Bloom 1 (NCNPR #16769) was the first ever titan arum to bloom in the University of Mississippi plant collections. This was also the first recorded bloom of titan arum in 2014 (http://en.wikipedia.org). The second inflorescence (bloom 2, #16771; Figures 1A–1C) was larger and taller than the first one. Its spathe measured 86 cm across (about 2.72 m in circumference) at the top. The middle part of the spathe was 1.04 m in circumference. The sterile part of the column, the appendix, was 1.22 m tall and had a circumference of 56 cm at the middle portion and 61 cm at the basal portion. The short and stout stalk of the inflorescence was 33 cm in circumference. Both the inflorescences reached their full blooms towards midnight. The carpels (female flowers) were receptive only for a short duration during anthesis and had ceased their receptivity by early morning of the following day. This was observed by the presence of sticky exudates on the stigma. The dehiscence of stamens happened 1 day (in the first bloom) or 2 days (in case of the second bloom) later, in the morning hours when the carpels of the same inflorescence were not receptive. Thus, the male and female flowers of the same inflorescence are spatially as well as functionally separated in order to avoid self-pollination.

The characteristic rotting-meat odor of the inflorescence began early in the evening and gradually increased to its peak towards midnight during the female flowering phase. At that time the stench was so strong that it could be smelled several yards away in spite of the fact that the plant was kept in a closed facility. In natural habitats the odor could possibly be far-reaching. The odor came mainly from the central column and lower part of the spathe. Since the plant was kept in a closed greenhouse in a nonnative geographical location, only a few flies, ants, and roaches were observed visiting the bloom. The spathe started closing during the following day of anthesis and the spathe as well as the appendix part of the column gradually shrank and eventually collapsed after a week.

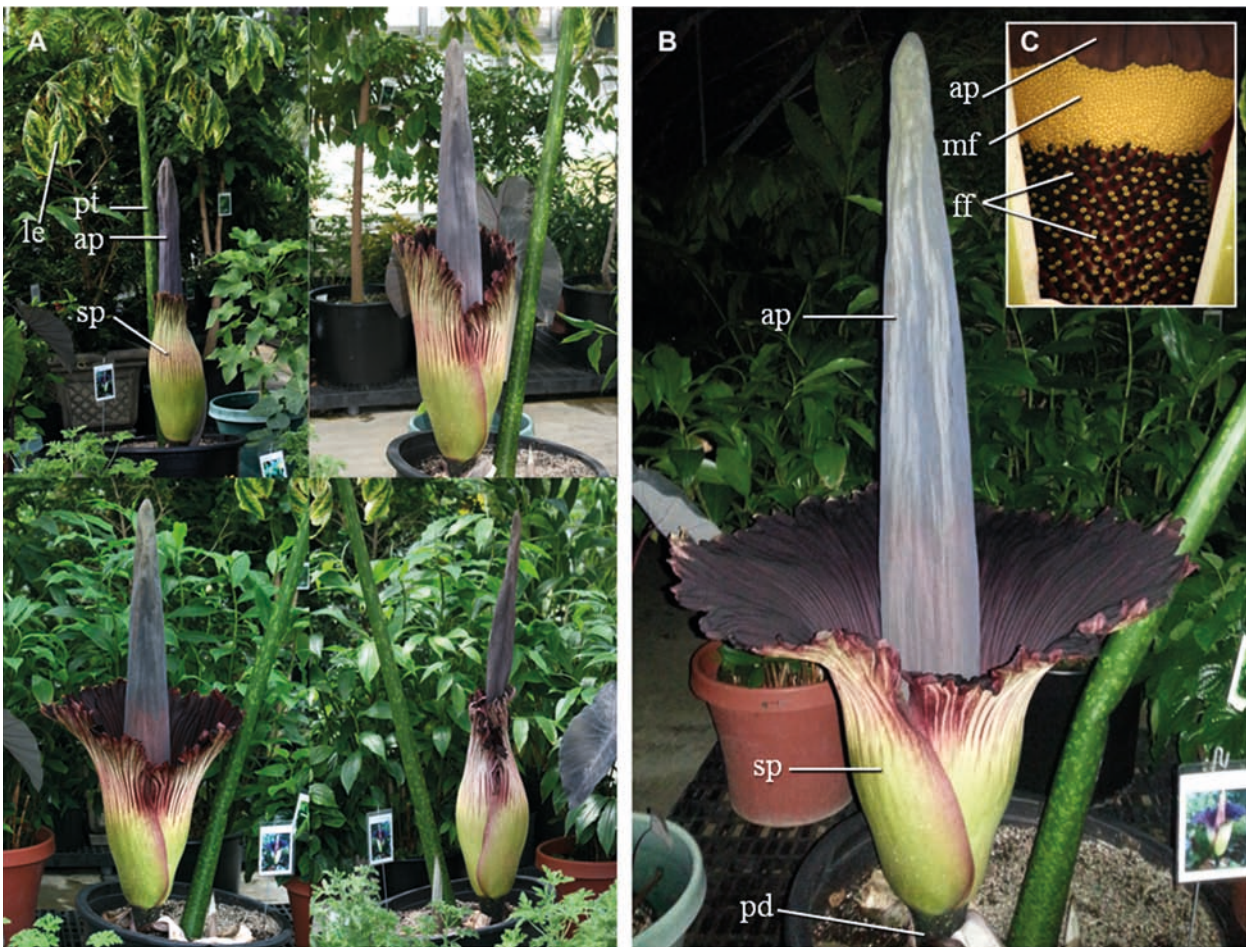

Figure 1. Pictures of *Amorphophallus titanum* inflorescence. A- Stages of titan arum flowering; B- fully opened inflorescence; C- lower part of spathe cut open to show the stamens and carpels (representing male and female flowers, respectively) studded on the lower part of the spadix. ap- appendix, ff- female flowers/carpels, le- leaf, mf- male flowers/stamens, pd- peduncle, pt- petiole, sp- spathe.

3.2. Chemical analysis of the floral scent

In the present study, HS-SPME was used to collect and determine the volatile constituents from various parts of the titan arum inflorescence such as the appendix, male and female flowers, and spathe (Table). Following the HS-SPME collection of the volatile compounds, GC-MS was used to identify the analytes from the headspace needle. A total of 25 constituents, representing 76.2%–93.9% of the total analyte composition, were identified. The volatile profiles of the appendix, male flowers, female flowers, and spathe were clearly different from each other. Isovaleric acid (21.6%), butyric acid (17.0%), benzyl alcohol (16.2%), γ-butyrolactone (12.1%), 3-hydroxy-2-butanone (5.9%), and benzaldehyde (4.4%) were the dominant volatile components in appendix. Volatiles from the spathe consisted mainly of butyl acetate (44.5%), 3-hydroxy-2-butanone (12.2%), ionol (5.7%), and methyldihydrojasmonate (2.4%). The main differences in the concentrations of volatile compounds between male and female flowers were observed for γ-butyrolactone (27.0% and 0.1%), tetradecane (13.4% and 19.9%), 4-hydroxy-4-methyl-2-pentanone (10.5% and 13.0%), ionol 2 (9.0% and 8.3%), benzyl alcohol (6.1% and 3.0%). 3-hydroxy-2-butanone (3.3% and 10.6%), 2-ethyl hexanol (2.0% and 7.7%), and phenol (2.9% and 4.3%), respectively. Isovaleric acid (4.0%), α-terpinyl acetate (2.8%), linalool (2.1%), 2-phenylethanol (1.7%), and nonanal (0.1%) were found only in the male flowers, while tridecane (4.4%) and long-chain *n*-alkanes (C_{25} to C_{28}) such as pentacosane (3.8%), hexacosane (5.1%), heptacosane (6.8%), and octacosane (6.9%) were only present in the female flowers.

In the current study, a total of 25 volatile compounds including six alkanes, three ketones, three phenols, two acids, two esters, two aromatic alcohols, two terpenes, one lactone, one fatty alcohol, one aromatic aldehyde, one alkyl aldehyde ester, and one pyrazine were identified. These compounds, apart from other previously reported (Shirasu et al., 2010; Fujioka et al., 2012) major odorants such as dimethyl disulfide, dimethyl trisulfide, and trimethylamine, could contribute to the characteristic putrid odor of the corpse flower. As per the volatile composition given in the Table, we found qualitative as well as quantitative differences among the various plant tissues. Some of these volatile compounds have fruity or pleasant odors, like butyl acetate (sweet floral (Giri et al., 2010)), 4-hydroxy-4-methyl-2-pentanone (sweet floral (Lasekan and Abbas, 2010)), benzyl alcohol (sweet floral (Liu et al., 2014)), benzaldehyde (almond odor (Liu et al., 2014)), 2-phenoxyethanol (flowery, fresh (Selli et al., 2009)), linalool (fresh floral (Katsuno et al., 2014)), methyl dihydrojasmonate (jasmine [www.flavornet.org]), 2-ethyl hexanol (green, rosy (Giri et al., 2010)), while some of the compounds have unpleasant or 'off' odors such as trimethyl pyrazine (roasted/baked/burned/musty (Giri et al., 2010)), butyric acid (cheese [www.flavornet.org]), isovaleric acid (cheese/feet/sweat/milky (Ubeda et al., 2012)), γ-butyrolactone (rancid/varnish [www.flavornet.org]), phenol (feces (Johnson and Jürgens, 2010)) 3-hydroxy-2-butanone (buttery (Liu et al., 2014), nonanal (beefy/buttery (Shi et al., 2013)), and α-terpinyl acetate (waxy [www.flavornet.org]). Some of the volatile compounds were only present in one of the floral parts, e.g., butyl acetate, ionol, and methyl dihydrojasmonate were only found in the spathe; tridecane and alkanes in the female flowers; trimethyl pyrazine, benzaldehyde, and butyric acid in the appendix; and linalool and α-terpinyl acetate in the male flowers.

3.3. Anatomy

Spathe/Bract (Figures 2A–2P): The lower part of the spathe is thick and fleshy and gradually becomes thin and papery towards the apex. The spathe is purplish inside (adaxial; Figure 2A) and greenish on the outside (abaxial; Figure 2B). The outer epidermis is covered with thick, irregularly striated cuticle (Figures 2B, 2C). The cells are polygonal or isodiametric, with straight or slightly curved anticlinal walls. Stomata (Figures 2B–2D) are frequent, of parasitic or anomocytic type, measuring 37–40 × 34–45 μm, positioned at or slightly below the level of the epidermis. Transverse section (TS) of the fleshy lower part of the spathe (Figures 2E–2M) shows the outer epidermis, outer cortex, and a wide aerenchyma region in the middle, followed by inner cortex and inner epidermis. The outer cortex is several cells wide; cells polygonal, with thin walls, dense cytoplasm, chloroplastids, and large nuclei. Idioblast cells filled with yellowish homogeneous or brown granular content are abundant. Crystal idioblasts containing raphide bundles (Figure 2J) are also abundant in the cortex, more so in the outer layers of cells. Raphide bundles measure 55–95 μm long and 27–42 μm in diameter. Small cells containing solitary cluster crystals of 18–22 μm in diameter are common in the outer cortex.

The middle region of the spathe, in TS view, is composed of networks of aerenchyma cells enclosing large air spaces (Figures 2G–2I). A few vascular bundles are randomly distributed throughout the aerenchyma region, which is followed by the inner cortex of polygonal cells. Oil droplets are rarely observed. Vascular bundles, collenchyma, and raphide crystals are not observed in the inner cortex. The inner epidermal cells are papillate. Stomata are not observed on the inner epidermis. The cuticle is thick but not prominently striated. The inner hypodermis and the cells of a few layers of the inner cortex contain anthocyanin pigments giving a purple or reddish brown color to the inner surface of the spathe. Sclerenchyma cells are not observed in the spathe. Cluster crystals are common in the cortical cells close to the inner epidermis. TS of the upper

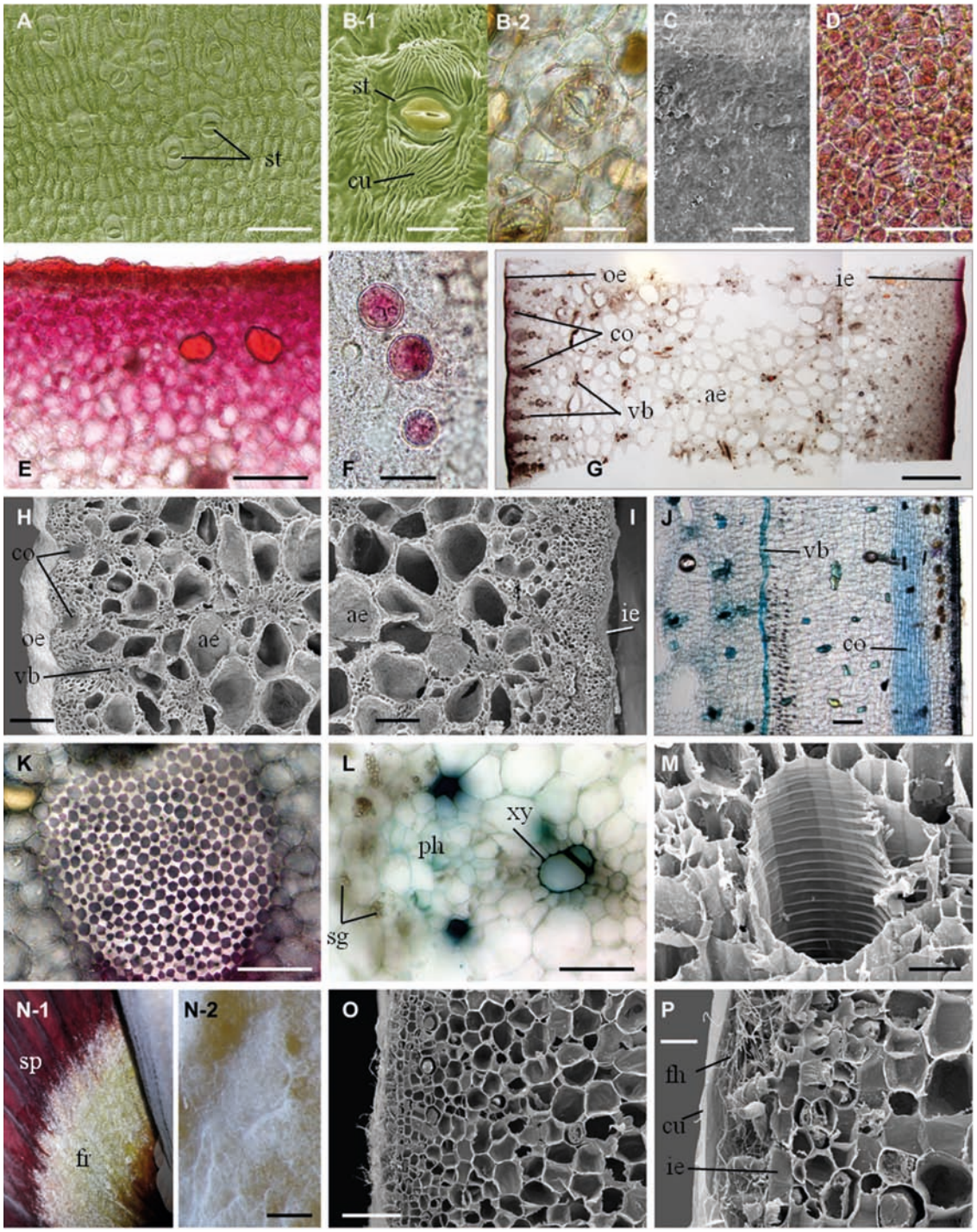

Figure 2. Anatomy and micromorphology of spathe of *Amorphophallus titanum* (B, C, H, I, M, O, P: SEM; A, D–G, J–L: light microscopy; N: photographs). A- Inner epidermis; B- outer surface of spathe showing striated cuticle and stomata; C and D- stomata; E- portion of spathe in TS showing pigmentation in inner epidermis and cortex; F- anthocyanin pigments; TS of lower part of spathe showing groups of collenchyma near outer epidermis, aerenchyma with large air spaces in the middle and pigmented inner epidermis; H- TS of spathe through outer surface; I- TS through inner surface; J- LS through outer surface; K- collenchyma; L- vascular bundle; M- metaxylem element showing secondary thickening; N-1- inner view of the spathe showing fungal growth; N-2- close-up view of fungal colonies; O & P- transections through fungal region of spathe showing fungal mycelia on the inner surface as well as in the subcuticular spaces of inner epidermis. ae- aerenchyma, co- collenchyma, cu- cuticle, fh- fungal hyphae, fr- fungal region, ie- inner epidermis, oe- outer epidermis, ph- phloem, sg- starch grains, sp- spathe, st- stomata, vb- vascular bundle, xy- xylem. *Bars*: B, E, K, L, O = 100 µm; C, F, M, P = 20 µm; A, D = 50 µm; G = 2 mm; H, I = 500 µm; J = 200 µm; N-2 = 250 µm.

part of the spathe shows features similar to those of the lower part but narrower in size.

Several columns of collenchyma of 200–500 µm in diameter traverse the outer cortex at regular intervals, each capping a vascular bundle (Figures 2G, 2H, 2J, 2K) as seen in cross-sectional view. Vascular bundles (Figure 2L) are collateral; xylem occurring towards the center of the spathe and phloem facing the epidermis. Xylem (Figures 2L, 2M) consists of usually 1–2, rarely 3–8 xylem elements with spiral or circular thickening, measuring up to 80 µm in diameter. Metaxylem elements eventually degenerate to form a xylemic canal, which is often filled with a yellow substance. Phloem consists of a few sieve elements and parenchyma. A few parenchyma cells that are capping the phloem contain starch grains, which are solitary or in groups of 4–8, measuring 4–9 µm in diameter.

Fungal growth, appearing as a cottony white coating, was observed on the inner surface of the lower part of the spathe. Its function and relationship with the inflorescence, if any, is not known. The fungal mycelia were observed to be present only on the epidermal surface and were not observed entering into the cells (Figures 2N–2P). Spores of this fungus were not observed in the collected samples so the identity of the fungus could not be established.

Appendix/Column (Figures 3A–3F): The appendix is purplish outside (Figure 3A). TS of the appendix is semicircular in outline and has the epidermis, a wide cortex, and the central wide space traversed by networks of aerenchyma (Figures 3B, 3C). The epidermis is unilayered, composed of tabular cells filled with anthocyanin pigment (Figure 3D), and covered externally by a thick cuticle layer. Stomata are not observed in the epidermis of the appendix. The hypodermis is uniseriate with the cells filled with anthocyanin. The cortex is several cells wide, traversed occasionally by small vascular bundles. Cells containing yellowish brown granular substance are occasional (Figures 3E-1, 3E-2). Crystal idioblasts containing raphide bundles are occasional in the outer cortex and are rarely found in the aerenchyma. The aerenchyma region is supplied with a few vascular bundles. The degenerating metaxylem elements form xylemic canals, which are often filled with yellow contents (Figure 3F).

Stamens/male flowers (Figures 3G–3L): In titan arum, the male flowers are represented by stamens each with a bithecal anther and a short and stout filament (Figure 3G). Anthers are 2–3 mm high, 2.5–3 mm wide, and 1.5–2 mm thick, and the filament is 1.2–1.4 mm long. Anthers open by terminal slits to disperse the pollen grains. In TS (Figures 3H–3K), the anther shows four pollen sacs of about 0.5 mm in diameter. The epidermis is uniseriate, covered externally with a thin cuticle; the cells radially slightly elongated, 48–56 × 20–42 µm, containing oil droplets; the outer tangential walls are slightly thickened. Starch cells are 3–5-layered, thin-walled, and slightly tangentially elongated; raphide crystals are occasionally found in this region. The endothecium is fibrous and encircles the pairs of pollen sacs. It is constituted by 4–6 layers of lignified and radially elongated cells measuring 20–110 × 14–45 µm, showing radial or rarely spiral or reticulate thickenings. The cells of the middle layers are tangentially elongated. The connective tissue forms a wide wall between the two anther lobes and is supplied with a few small vascular bundles. Starch grains are abundant, solitary, 1–3 µm in diameter. The pollen grains (Figure 3L) are usually spherical or ovoid-subglobose, measuring 45–75 µm in diameter. The surface of the pollen grain is psilate and inaperturate.

Carpels/female flowers (Figures 4A–4K): The carpel consists of a stigma, style, and ovary. The stigma (Figures 4A, 4B) is subspherical, shallowly bilobed at apex, ca. 2 mm high and 3 mm wide, clothed with large unicellular stigmatic papillae. Stigmatic papillae are partially immersed in an exudate secretion that they produce, a characteristic feature of wet stigma (Heslop-Harrison, 1981; Giordano, 1999). The style is cylindrical, purple, and 2–2.8 mm in diameter (Figures 4A, 4C). TS of style (Figures 4D–4I) shows the following characteristics: epidermis is unilayered; the cells are papillate and covered externally with striated cuticle (Figures 4F, 4G). The cortex is made up of several layers of isodiametric cells and the outermost layers of cells are filled with anthocyanin. Many vascular bundles (Figure 4H) are arranged in the middle of the cortex forming an interrupted ring. A few additional bundles occur randomly in the inner part of the cortex. Xylem elements are few, 5–18–80 µm in diameter, spirally thickened and lignified; phloem consists of a few sieve elements and polygonal parenchyma. A central mucilage canal (Figure 4I) that runs through the style and ovary, of about 160 µm in diameter in the style and 230–300 µm wide in the ovary, is lined by a few layers of collapsed cells. A few idioblasts containing raphide bundles occur in the outer part of the cortex.

Ovary is about 5 mm in diameter containing 2–3 ovules. TS of ovary (Figures 4J, 4K) is circular in outline and has 2–3 large ovule chambers near the center. The epidermal cells are strongly papillate and covered externally by striated cuticle. The cortex is wide, made up of several layers of polygonal parenchyma; outermost layers of cells contain anthocyanin. The cortex harbors numerous raphide-containing idioblasts of 75–95 × 50–65 µm. Two types of raphide crystals (types I and II) are observed. The middle region of the cortex is traversed by several vascular bundles occurring in two irregular interrupted rings. The ovule chambers are lined by a layer of palisade-like cells.

Crystals of calcium oxalate: Clusters crystals (Figures 5A, 5B) and raphides (Figures 5C–5J) of calcium oxalate

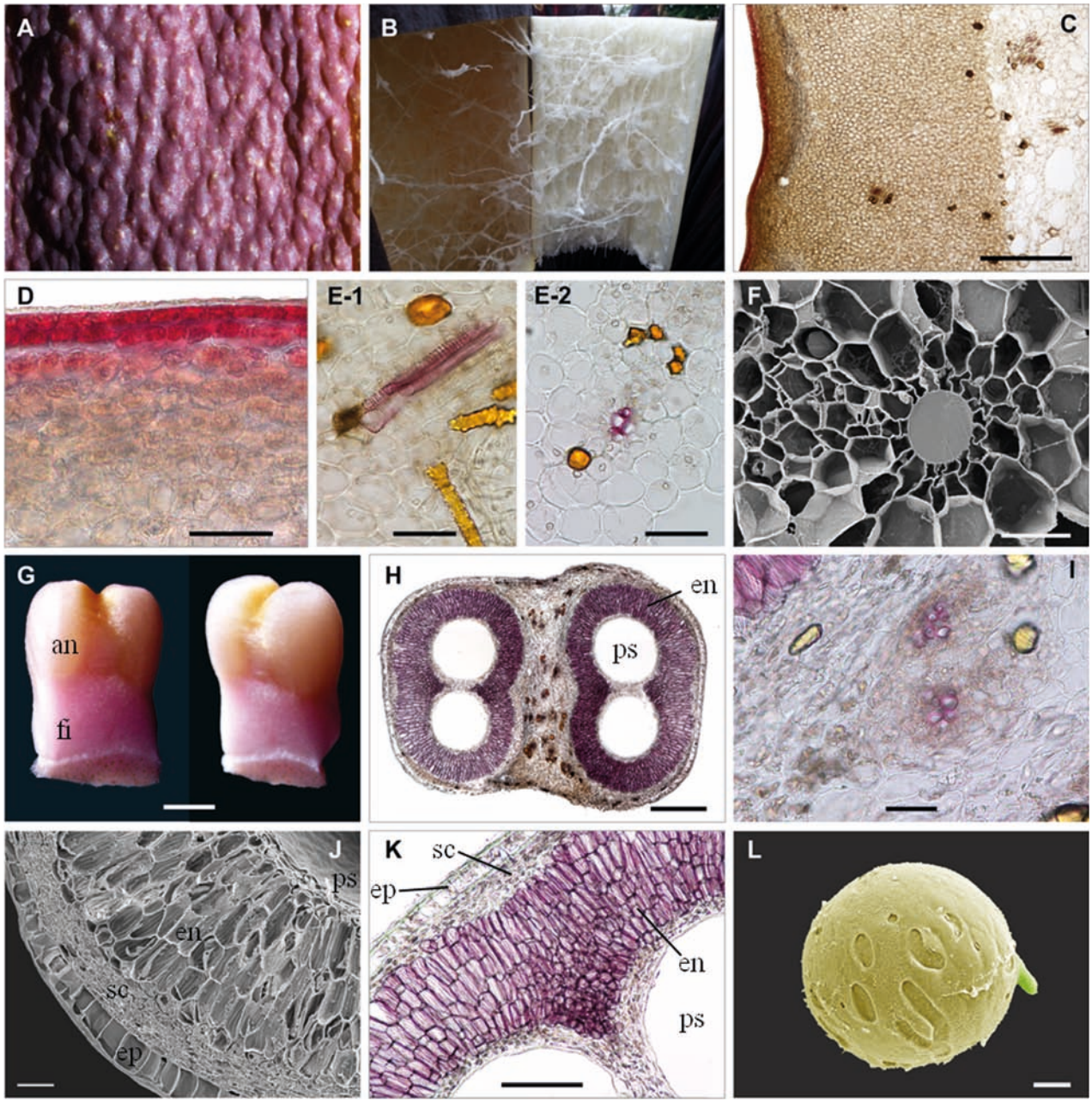

Figure 3. Morphoanatomy of floral parts of *Amorphophallus titanum* (A, B, G: photographs; F, J, L: SEM; C–E, H, I, K: light microscopy). A- Close-up view of appendix surface; B- a portion of appendix cut open to show the hollow inside traversed by aerenchyma; C–F- transections of appendix showing regions of outer parenchyma and inner aerenchyma (C), epidermis with anthocyanin pigments (D), tannin-containing cells and canals associating with vascular bundles (E-1 and E-2) and xylemic cavity filled with tannin substance (F). G- Stamens; H–K- transection of an anther; L- a germinating pollen grain. an- anther, en- endothecium, ep- epidermis, fi- filament, ps- pollen sac, sc- starch cells. *Bars*: C, H = 500 µm; D, F, J = 50 µm; E-1, E-2, I = 100 µm; G = 1 mm; K = 200 µm; L = 10 µm.

are present in various tissues of titan arum inflorescence. However, raphide crystals are more abundant in occurrence. Two types of raphide crystals are present: a) type I (*Psychotria* type, Figures 5E, 5F) crystals are about 60–90 µm long and 0.5–1 µm wide, with slender 4-sided body and pointed ends; and b) type II (*Lemna* type, Figures 5G–5J) raphide crystals are about 30–90 µm long and 2–2.5 µm wide, with a 4-sided body and pointed ends, solid in the middle, with two opposing grooves toward each end giving an 'H' shape in cross-section (Horner and Wagner, 1995; Raman et al., 2014). Some of the crystals have additional points on either side of the pointed ends

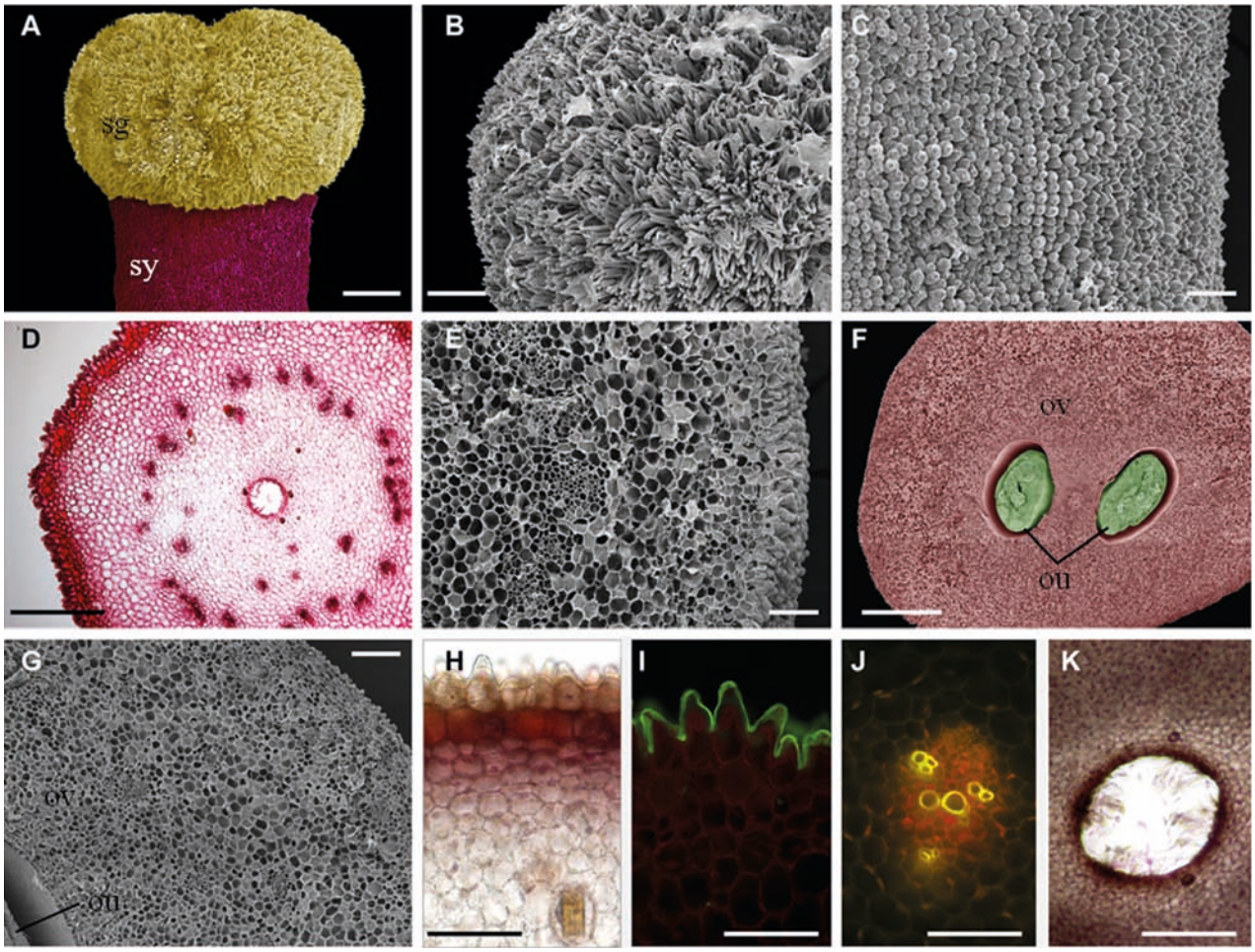

Figure 4. Morphoanatomy of pistillate flower of *Amorphophallus titanum* (A–C, E, J, K: SEM; D, F, I: light microscopy; G, H: fluorescent microscopy). A- Stigma with a portion of style; B- stigma showing finger-like projections; C- style surface showing papillate epidermis; D, I- TS of style (TS of style showing papillate epidermis (D–G), cuticle layer (G), vascular bundle (H), and the central mucilage canal (I)); J- TS of ovary and ovules; K- a portion of ovary in TS. ou- ovule, ov- ovary, sg- stigma, sy- style. *Bars*: A, D = 500 µm; B, K, I = 200 µm; C, E, F, G, H = 100 µm; J = 1 mm.

(Prychid et al., 2008). Numerous crystals of raphides are found freely distributed in the stigmatic fluid (Figure 5J).

4. Discussion

In the present work, macro- and microscopy of titan arum inflorescence were analyzed and the volatile composition of the floral scent was characterized. Detailed descriptions of the spathe, appendix, male flowers, and female flowers, illustrated with light and scanning electron micrographs, were prepared and included in this paper. Calcium oxalate crystals of druses and raphides were observed. Two types of raphides, namely the *Psychotria* type and *Lemna* type, were recognized. Colonization of fungi in the bloom was observed.

Previous studies (Korotkova and Barthlott, 2009) reported that the male flowering phase occurred the night following the female flowering phase. However, it was observed during the present study that the male flowering phase occurred the following morning or, in the case of the second flower, the next morning. The surface of the pollen grain is psilate and inaperturate as in most of the species of the tribe *Amorphophallae* (Giordano, 1999). According to Giordano (1999), the pollen wall consists of three distinguishable layers: ectexine, endexine, and intine.

Using HS-SPME and GC-MS systems, it was found that the odor of the corpse flower was due to a complex mixture of volatile compounds produced by different floral parts. The modified HS-SPME method revealed the presence of strongly unpleasant odor compounds such as butyric acid, γ-butyrolactone, isovaleric acid, phenol, and trimethyl pyrazine in the appendix part of the inflorescence that could contribute to the carrion-like odor of the bloom. Additionally, there were some sweet-smelling compounds observed, such as butyl acetate, 4-hydroxy-4-methyl-

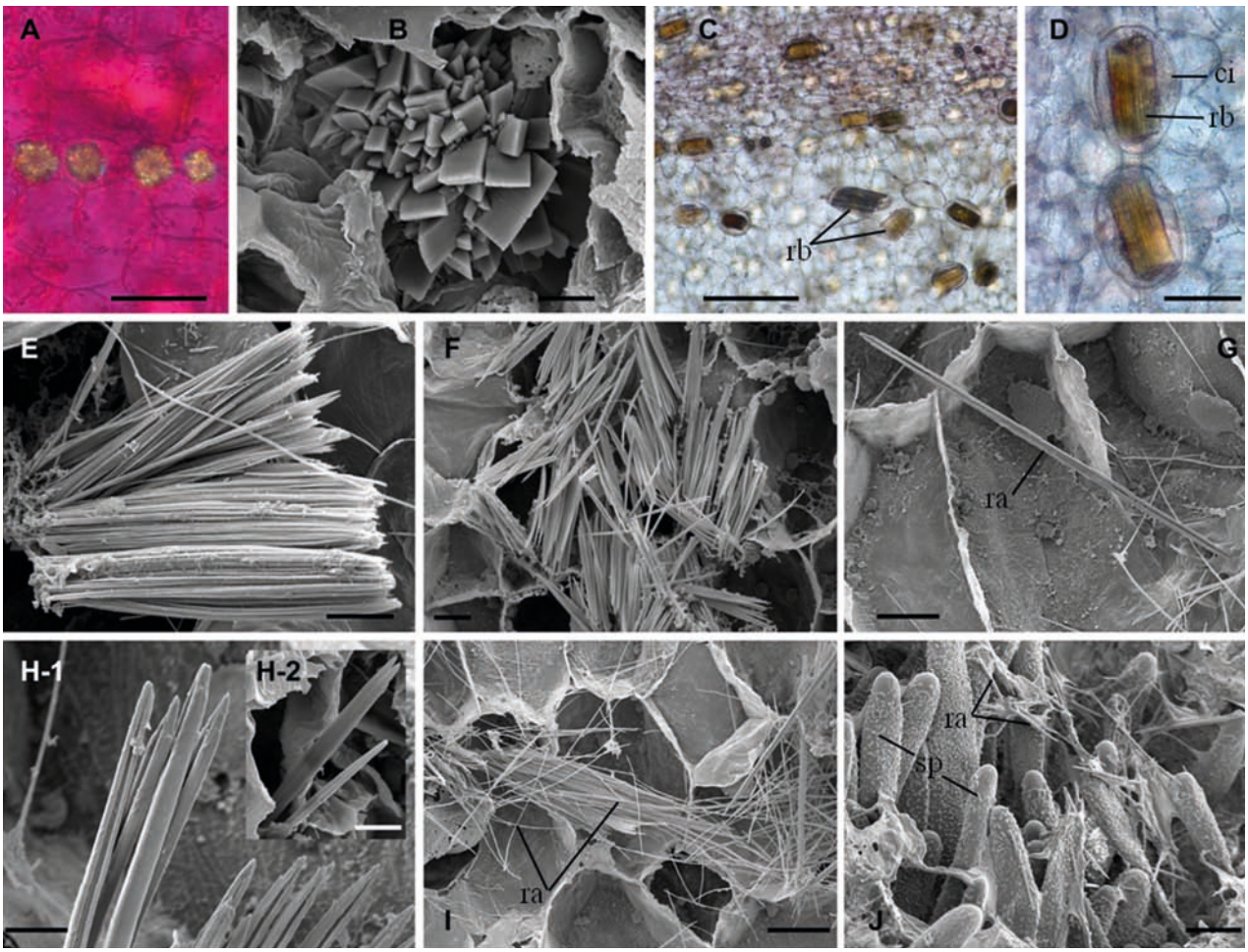

Figure 5. Crystals of calcium oxalate in *Amorphophallus titanum* inflorescence (A: polarized light microscopy; C, D: light microscopy; B, E–J: SEM]. Cluster crystals (A, B) and raphides (C–J) are common in the spathe and female flowers. Slender raphides of *Psychotria* type (E, F) and stout, *Lemna* type needles (G–J) are observed in the female flowers. Image J shows raphide crystals dispersed in the stigmatic fluid. ci- crystal idioblast, ra- raphide crystal, rb- raphide bundle, sp- stigmatic papillae. *Bars*: A, D = 50 µm; B, I-1 = 5 µm; C = 200 µm; E, G, H, I-2 = 10 µm; F, J = 20 µm.

2-pentanone, 2-ethyl hexanol, linalool, benzylalcohol, 2-phenoxyethanol, and methyl dihydrojasmonate, which could help attract the nectar- and pollen-seeking insect pollinators. The fermented-like smelling volatile compound 3-hydroxy-2-butanone (acetoin) was reported as a reward to pollinators (Steenhuisen et al., 2010), and in the present study, acetoin was found to be present in all parts of the titan arum inflorescence.

The presence of dimethyl oligosulfides as major odorants in malodorous flowers in the family Araceae is well known. A few studies were previously published on the chemical identity of the floral scent of titan arum. Shirasu et al. (2010) performed GC-MS-olfactory analysis of the inflorescence using a Carboxen/polydimethylsiloxane (CAR/PDMS)-coated SPME fiber. They reported dimethyl trisulfide as the main odorant during the opening of the spathe and trimethylamine during the end of flowering. In the same study, the authors also identified methyl thiolacetate, 3-methyl butanal, acetic acid, and isovaleric acid (Shirasu et al., 2010). In another study, Fujioka et al. (2012) analyzed floral odors from titan arum using an FF-2A fragrance analyzer. They described the flower smell as a mixture of methyl mercaptan and propionic acid. These compounds, except for isovaleric acid, were not detected by the present polydimethylsiloxane/divinylbenzene (PDMS/DVB)-coated SPME fiber, which, however, detected more volatile compounds with molecular weights between *m/z* 50 and 300. Fibers coated with CAR/PDMS seemingly detect gases and compounds with low molecular weights (MW 30–225) (www.sigmaaldrich.com). The present PDMS/DVB fiber did not adsorb gases and small molecules, but it detected a wide range of compounds with different polarities and molecular masses. This indicates that use of multiple types of fibers and analytical methods

is necessary in order to obtain a more complete picture of the volatile composition. SPME is simple, fast, solvent-free, and useful technique for fragrance compounds; however, absorption of the key components strongly depends on the SPME fiber coatings.

It is well known that volatile compounds play an important role in plant–insect interactions (Heiduk et al., 2010). They evolve to attract pollinators or invite parasites or repel arthropods. Levin et al. (2001) reported that acyclic terpene alcohols (linalool, nerolidol), aromatic alcohols (benzyl alcohol, 2-phenylethanol, and their esters), lactones, jasmonates, tiglates, and nitrogen-bearing compounds are more characteristic for moth-pollinated flowers. Each fragrant compound behaves differently to different insects and also individual compounds could act differently when they are within volatile mixtures. For example, while 3-hydroxy-2-butanone (acetoin) attracted *Drosophila melanogaster*, butyl acetate is incorporated in the volatile mixture used for trapping bedbugs (Green, 2014). Benzyl alcohol together with 2-phenyl ethanol and phenyl aldehyde attract honey bees (Filella et al., 2011). Chen et al. (2012) found that butyl acetate was the major volatile compound from the inflorescence of *Buddleja officinalis* and the flower was visited mostly by ants and butterflies.

It was interesting to note that relatively short-chain alkanes [tridecane (C13) and tetradecane (C14)] together with long-chain alkanes [(C25), hexacosane (C26), heptacosane (C27), and octacosane (C28)] accumulated mainly in the female flower (Table). Alkanes are well known to form much of the epicuticular wax in the plants (Kundu and Sinhababu, 2013) and the functions of these aliphatic compounds were reported to reduce water loss of the epidermis, reduce water retention on the plant surfaces, control leaf temperature, protect the plant from ultraviolet radiation, and defend the plant against pathogens and insects (Nadakuduti et al., 2012; Kundu and Sinhababu, 2013; Guo et al., 2014). Although alkanes do not have any particular odor, they seem to play an important role as physical barriers against pathogens and/or insects as well as in maintaining the balance of temperature, humidity, and dehydration in the plant.

Carrion flies, sweat bees, and dung beetles are reported to be the main pollinators of this carrion flower (Gandawijaja et al., 1983). Van der Pijl (1937) reported a sylphid beetle (*Diamesus osculans*) and a staphylinid beetle (*Creophilus villipennis*) in the inflorescence of titan arum. The floral odor of titan arum may attract different pollinators in different areas (Barthlott and Lobin, 1998). The full bloom along with emission of the highest intensity of the odor combined with generation of heat occurs late in the night in order to attract a unique group of nocturnal insects. The flesh-colored floral parts with the characteristic odor combined with the warmth rendered by the thermogenesis process (Barthlott et al., 2009; Korotkova and Barthlott, 2009) are perfect rewards for these pollinators and this multifaceted adaptation of titan arum is an excellent example of biomimicry. This also explains the incredible and intricate behavior of titan arum for achieving successful pollination.

In conclusion, the floral scent chemistry and concentration of the volatile compounds recorded during the present study add to the existing knowledge and illustrate the wide spectrum of volatile composition of titan arum floral scent. The quality and quantity of the scent's volatile composition may also vary between flowers, places, and different times of flowering. In other words, the volatile compounds produced by the flower in the evening might be different from those produced during full bloom at midnight and so in the following hours. Therefore, more comprehensive studies involving multiple plants at different geographical locations and at different phases of flowering using a wide range of sampling with different types of SPME fibers are required in order to fully characterize the composition of the complex odor of titan arum bloom. These studies will also throw more light on the behavior of titan arum flowering and the biology of its pollination.

Acknowledgments

We appreciate Dr Louis Ricciardiello, in Gilford, New Hampshire, for his generous donation of the titan arum seeds. The plants were raised and cared for by Aruna Weerasooriya, Edward Lowe, Derek Oglesby, and Lal Jayaratna at the Maynard W. Quimby Medicinal Plant Garden, University of Mississippi. This research was supported by USDA-ARS Grant No. 56-6402-1-612, a Deployed War-Fighter Protection Research Program grant funded by the U.S. Department of Defense through the Armed Forces Pest Management Board.

References

Barthlott W, Lobin W, editors (1998). *Amorphophallus titanum* - Tropische und subtropische Pflanzenwelt, Band 99. Stuttgart, Germany: Franz Steiner Verlag (in German).

Barthlott W, Szarzynski J, Vlek P, Lobin W, Korotkova N (2009). A torch in the rain forest: thermogenesis of the titan arum (*Amorphophallus titanum*). Plant Biol 11: 499-505.

Chen G, Gong W, Ge J, Dunn BL, Sun W (2012). Floral scents of typical *Buddleja* species with different pollination syndromes. Biochem Syst Ecol 44: 173-178.

Endress PK, Baas P, Gregory M (2000). Systematic plant morphology and anatomy: 50 years of progress. Taxon 2000: 401-434.

ESO-2000 (1999). The Complete Database of Essential Oils. Huizen, the Netherlands: Boelens Aroma Chemical Information Service.

Filella I, Bosch J, Llusià J, Peñuelas A, Peñuelas J (2011). Chemical cues involved in the attraction of the oligolectic bee *Hoplitis adunca* to its host plant *Echium vulgare*. Biochem Syst Ecol 39: 498-508.

Fujioka K, Shirasu M, Manome Y, Ito N, Kakishima S, Minami T, Tominaga T, Shimozono F, Iwamoto T, Ikeda K et al. (2012). Objective display and discrimination of floral odors from *Amorphophallus titanum*, bloomed on different dates and at different locations, using an electronic nose. Sensors 12: 2152-2161.

Gandawijaja D, Idris S, Nasution R, Nyman L, Arditti J (1983). *Amorphophallus titanum* Becc.: a historical review and some recent observations. Ann Bot-London 51: 269-278.

Giordano C (1999). Karyological and palynological observations on *Amorphophallus titanum* (Becc.) Becc. ex Arcangeli (Araceae). Caryologia 52: 65-73.

Giri A, Okamoto A, Okazaki E, Ohshima T (2010). Headspace volatiles along with other instrumental and sensory analyses as indices of maturation of horse mackerel miso. J Food Sci 75: S406-417.

Green PW (2014). Volatile compounds from *Liposcelis bostrychophila* (Psocoptera: Liposcelididae) and their environment and their effects on settling behaviour. Biochem Syst Ecol 57: 81-89.

Guo N, Gao J, He Y, Zhang Z, Guo Y (2014). Variations in leaf epicuticular n-alkanes in some *Broussonetia*, *Ficus* and *Humulus* species. Biochem Syst Ecol 54: 150-156.

Hayat MA (2000). Principles and Techniques of Electron Microscopy: Biological Applications. New York, NY, USA: Cambridge University Press.

Heiduk A, Brake I, Tolasch T, Frank J, Jürgens A, Meve U, Dötterl S (2010). Scent chemistry and pollinator attraction in the deceptive trap flowers of *Ceropegia dolichophylla*. S Afr J Bot 76: 762-769.

Hejnowicz Z (2005). Unusual metaxylem tracheids in petioles of *Amorphophallus* (Araceae) giant leaves. Ann Bot-London 96: 407-412.

Hejnowicz Z, Barthlott W (2005). Structural and mechanical peculiarities of the petioles of giant leaves of *Amorphophallus* (Araceae). Am J Bot 92: 391-403.

Heslop-Harrison Y (1981). Stigma characteristics and angiosperm taxonomy. Nord J Bot 1: 401-420.

Horner HT, Wagner BL (1995). Calcium oxalate formation in higher plants. In: Khan SR, editor. Calcium Oxalate in Biological Systems. Boca Raton, FL, USA: CRC Press, pp. 53-72.

Johnson S, Jürgens A (2010). Convergent evolution of carrion and faecal scent mimicry in fly-pollinated angiosperm flowers and a stinkhorn fungus. S Afr J Bot 76: 796-807.

Joulain D, König WA (1998). The Atlas of Spectral Data of Sesquiterpene Hydrocarbons. Hamburg, Germany: EB-Verlag.

Katsuno T, Kasuga H, Kusano Y, Yaguchi Y, Tomomura M, Cui J, Yang Z, Baldermann S, Nakamura Y, Ohnishi T et al. (2014). Characterisation of odorant compounds and their biochemical formation in green tea with a low temperature storage process. Food Chem 148: 388-395.

Kite GC, Hetterschieid WL (1997). Inflorescence odours of *Amorphophallus* and *Pseudodracontium* (Araceae). Phytochemistry 46: 71-75.

Korotkova N, Barthlott W (2009). On the thermogenesis of the titan arum (*Amorphophallus titanum*). Pl Signal Behav 4: 1096-1098.

Kundu S, Sinhababu A (2013). Analysis of n-alkanes in the cuticular wax of leaves of *Ficus glomerata* Roxb. J Appl Nat Sci 5: 226-229.

Lasekan O, Abbas K (2010). Analysis of volatile flavour compounds and acrylamide in roasted Malaysian tropical almond (*Terminalia catappa*) nuts using supercritical fluid extraction. Food Chem Toxicol 48: 2212-2216.

Levin RA, Raguso RA, McDade LA (2001). Fragrance chemistry and pollinator affinities in Nyctaginaceae. Phytochemistry 58: 429-440.

Liu XS, Liu JB, Yang ZM, Song HL, Liu Y, Zou TT (2014). Aroma-active compounds in jinhua ham produced with different fermentation periods. Molecules 19: 19097-19113.

McLafferty FW, Stauffer DB, Stenhagen E, Heller SR (1989). The Wiley/NBS Registry of Mass Spectral Data. New York, NY, USA: Wiley.

Nadakuduti SS, Pollard M, Kosma DK, Allen C, Jr., Ohlrogge JB, Barry CS (2012). Pleiotropic phenotypes of the sticky peel mutant provide new insight into the role of CUTIN DEFICIENT2 in epidermal cell function in tomato. Plant Physiol 159: 945-960.

Prychid CJ, Jabaily RS, Rudall PJ (2008). Cellular ultrastructure and and crystal development in *Amorphophallus* (Araceae). Ann Bot 101: 983-995.

Raman V, Horner HT, Khan IA (2014). New and unusual forms of calcium oxalate raphide crystals in the plant kingdom. J Plant Res 127: 721-730.

Selli S, Prost C, Serot T (2009). Odour-active and off-odour components in rainbow trout (*Oncorhynchus mykiss*) extracts obtained by microwave assisted distillation-solvent extraction. Food Chem 114: 317-322.

Shi X, Zhang X, Song S, Tan C, Jia C, Xia S (2013). Identification of characteristic flavour precursors from enzymatic hydrolysis-mild thermal oxidation tallow by descriptive sensory analysis and gas chromatography-olfactometry and partial least squares regression. J Chromatogr B 913-914: 69-76.

Shirasu M, Fujioka K, Kakishima S, Nagai S, Tomizawa Y, Tsukaya H, Jin M, Manome Y, Touhara K (2010). Chemical identity of a rotting animal-like odor emitted from the inflorescence of the titan arum (*Amorphophallus titanum*). Biosci Biotech Bioch 74: 2550-2554.

Steenhuisen SL, Raguso R, Jürgens A, Johnson S (2010). Variation in scent emission among floral parts and inflorescence developmental stages in beetle-pollinated *Protea* species (Proteaceae). S Afr J Bot 76: 779-787.

Tasdemir D, Demirci B, Demirci F, Dönmez AA, Baser K, Rüedia P (2003). Analysis of the volatile components of five Turkish *Rhododendron* species by headspace solid-phase microextraction and GC-MS (HS-SPME-GC-MS). Z Naturforsch C Bio Sci 58: 797-803.

Ubeda C, San-Juan F, Concejero B, Callejon RM, Troncoso AM, Morales ML, Ferreira V, Hernandez-Orte P (2012). Glycosidically bound aroma compounds and impact odorants of four strawberry varieties. J Agr Food Chem 60: 6095-6102.

van der Pijl L (1937). Biological and physiological observations on the inflorescence of *Amorphophallus*. Recueil Trav Bot Neerl 34: 157-167.